

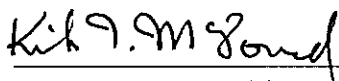
Renewal of Sponsored Research Grant RGFY9235

**Development of Detectors  
for the  
Superconducting Super Collider**

submitted to the  
*Texas National Research Laboratory Commission*

submitted by  
*Department of Physics  
Princeton University  
Princeton, New Jersey 08544*

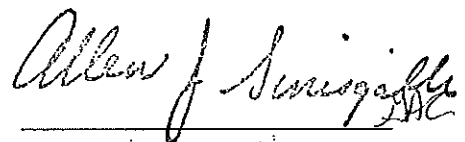
Covering April 1, 1993 to March 31, 1994



Kirk T. McDonald  
Professor of Physics  
Principal Investigator



A. J. Stewart Smith  
Professor of Physics  
Chairman, Physics Department



A. J. Sinisgalli  
Associate Provost

October 26, 1992



# Contents

<b>1</b>	<b>Description of the Research</b>	<b>1</b>
1.1	Introduction . . . . .	1
1.2	Proposed Research . . . . .	2
1.2.1	Radiators Transparent at 170 nm . . . . .	2
1.2.2	Preparation of High Quantum-Efficiency Photocathodes . . . . .	3
1.2.3	Cosmic-Ray Test Chambers . . . . .	3
1.2.4	Semitransparent Photocathodes . . . . .	4
1.2.5	LiF Substrate . . . . .	4
1.2.6	Spray-on Photocathodes . . . . .	5
1.2.7	Atmospheric-Pressure RICH Detectors with CsI . . . . .	5
1.2.8	CsI Photocathodes for Time-of-Flight Counters . . . . .	5
1.2.9	Beam Tests . . . . .	6
1.2.10	Infrastructure Support . . . . .	6
1.3	Research Personnel . . . . .	6
1.4	Methodology . . . . .	6
1.5	Relevance to the SSC . . . . .	7
1.6	Institutional Commitment and Sources of Additional Support . . . . .	7
1.7	Impact on Infrastructure of Science and Engineering . . . . .	7
<b>2</b>	<b>Research Accomplishments in FY91 and FY92</b>	<b>8</b>
2.1	Precision Straw-Tube Tracking . . . . .	8
2.2	Particle Identification with Fast RICH Counters . . . . .	8
2.2.1	Beam Test of a RICH Prototype . . . . .	8
2.2.2	Monte Carlo Simulation of the RICH Detector . . . . .	11
2.2.3	Measurement of Quantum Efficiency of CsI Cathodes . . . . .	13
2.2.4	Atmospheric-Pressure Operation . . . . .	15
2.2.5	Effect of Water Vapor on CsI Photocathodes . . . . .	18
2.3	Secondary Emission in Low-Density Semiconductor Films . . . . .	18
<b>3</b>	<b>References</b>	<b>19</b>
<b>4</b>	<b>Resumé of Kirk T. McDonald</b>	<b>23</b>

## List of Figures

1	Proposed test chambers for RICH and time-of-flight. . . . .	4
2	The prototype RICH detector. . . . .	9
3	Čerenkov events. . . . .	9
4	Spectrum of photoelectrons per Čerenkov ring. . . . .	10
5	Transmission of light in $C_6F_{14}$ . . . . .	12
6	Various efficiency distributions that enter the simulation. . . . .	13
7	The total number of detected photons. . . . .	14
8	The quantum-efficiency test chamber. . . . .	15



9	Quantum efficiency of CsI with isobutane and ethane gases. . . . .	16
10	Light transmission in methane, ethane and isobutane. . . . .	16
11	Quantum efficiency of CsI with He gas mixtures. . . . .	17
12	Sensitivity of He gas mixtures to minimum-ionizing particles. . . . .	18
13	Recovery of CsI photocathodes after exposure to water. . . . .	19
14	First setup for study of secondary emission. . . . .	20
15	Second setup for study of secondary emission. . . . .	20
16	Results on secondary emission in low-density CsI films. . . . .	21



# 1 Description of the Research

## 1.1 Introduction

Particle identification is essential for experiments that plan to study  $CP$  violation in the  $B$ -meson system. The Superconducting Super Collider is the ultimate ' $B$  factory,' offering the best combination of high rates ( $\gtrsim 10^{12}$   $B$ 's per year) and good signal to noise (roughly 1 event in 50 at the SSC is expected to contain a  $B$  particle). However, improved detector elements are required to profit from this splendid physics opportunity.

There are many  $B$ -meson decay modes that should exhibit  $CP$  violation, but the most precise information will come from the class of neutral  $CP$ -self-conjugate decay modes, such as  $B \rightarrow J/\psi K_S^0$ . The analysis of  $CP$  violation in such decays requires knowledge of whether a  $B$  or  $\bar{B}$  produced the final decay products, and consequently the other  $B$  in the event must be 'tagged' as a  $\bar{B}$  or  $B$ . The charge of the  $K$  meson from  $B$  decays with the quark decay chain  $b \rightarrow c \rightarrow s$  will tag with high efficiency the conjugation of the parent  $B$  meson. Čerenkov detectors provide a method of separating charged  $\pi$ 's from  $K$ 's and will therefore be important in the tagging process.

Several others methods have been proposed to measure  $CP$ -violating phases in  $B$ -meson decays that are also free of ambiguities due to strong interactions [1]. Most of these involve decays to non- $CP$  eigenstates that contain  $D^0$  mesons. The latter decay to final states containing a charged Kaon with high probability, so Kaon identification is also vital for these additional measurements of  $CP$  violation.

The Ring Imaging Čerenkov (RICH) detector [2] provides  $\pi$  and  $K$  identification over a greater momentum range than any other technique available. However, large RICH systems are difficult to build and operate at high rates and with high yields of photoelectrons.

RICH detectors using photomultiplier tubes perform well but are expensive to implement on a large scale, and insert a significant amount of material in the particles' path.

The largest and most ambitious existing RICH systems, such as those at SLD [3] and Delphi [4], use a readout based on the photosensitive gas TMAE. For operation at atmospheric pressure a buffer gas is present, which typically is overly sensitive to minimum-ionizing particles and renders the detectors unstable at high gas gains. To achieve good quantum efficiency the TMAE gas volume is large, leading to long collection times for the photoelectrons. The photoabsorption length, and hence the collection time can be shortened by raising the temperature of the TMAE gas [5, 6]. However, the obvious operational and mechanical difficulties are such that at present no large system is proposed using this approach.

A variation on the TMAE gas detector employs a multistep-avalanche chamber where several stages of gain achieve high amplification while minimizing instabilities to photon feedback. These detectors still require heated TMAE gas to achieve a high quantum efficiency with a thin photosensitive layer [5, 6, 7].

In the present work we explore the use of low-pressure gas chambers with a solid cesium-iodide (CsI) photocathode. Such cathodes have been studied since the 1950's [8], and it is established under certain circumstances they deliver high quantum efficiency, but their performance is readily degraded by absorption of water vapor [9].

In the last two years the work of the Anderson group at Fermilab [10, 11, 12], the Charpak group at CERN [13, 15], the Ypsilantis group at Collège de France [14], and the Breskin group



in Israel [16, 17] indicates great promise for RICH detectors using high-quantum-efficiency CsI photocathodes. The fast time response of the solid photocathode [10, 15] enables a RICH detector to be designed with a pad-chamber readout which will be appropriate for use at high-luminosity hadron colliders and  $B$  factories. Low-pressure operation renders the detector almost blind to minimum-ionizing particles, so they can be operated at very high gas gain. Furthermore, there is little loss of photoelectrons due to backscattering onto the cathode [19], and ion collection times are minimized as the mean free path is long. CsI cathodes coupled to low-pressure chambers show good quantum efficiency for wavelengths up to  $\approx 210$  nm, so can be used with relatively inexpensive quartz windows. The resulting narrow sensitivity in wavelength (170-210 nm) minimizes chromatic dispersion as needed for good  $\pi/K$  separation.

In FY92 we built and tested a parallel-plate, low-pressure RICH detector with a CsI photocathode evaporated onto cathode pads [18]. We believe this constitutes the first observation of Čerenkov rings in a detector with a CsI photocathode. This proposal is for continuation of that research program in FY93.

## 1.2 Proposed Research

We will continue our work in progress on various aspects of the RICH detector, and inaugurate several new programs of study. In brief these are:

1. Search for radiators with good transparency at 170 nm.
2. Systematic study of preparation of photocathodes with high quantum efficiency.
3. Construction of a pair of large-area single-pad test chambers for use with cosmic rays.
4. Study of the viability of semitransparent CsI photocathodes.
5. Study of possible gain in quantum efficiency by use of a LiF substrate.
6. Investigation of spray technology for production of photocathodes.
7. Construction of prototype atmospheric-pressure RICH detectors with CSI photocathodes.
8. Study of low-density CsI cathodes for use in time-of-flight counters.
9. Testing of various photocathode detectors at BNL in summer '93.

### 1.2.1 Radiators Transparent at 170 nm

Thus far RICH detectors with liquid radiators have used  $C_6F_{14}$  for the radiator, as this has good uv transparency and the lowest index of refraction of any reasonably stable liquid at room temperature. A low index is considered desirable to keep the Čerenkov angle from approaching  $90^\circ$  after exiting the liquid. Recall that

$$\sin \theta_{\text{vacuum}} = n \sin \theta_C = \sqrt{n^2 - 1},$$



so that for  $n > \sqrt{2}$  the Čerenkov light is internally reflected at the liquid-window-vacuum interface. Furthermore,  $n$  should not be too close to  $\sqrt{2}$  to limit chromatic dispersion. Also, a higher index leads to a lower maximum momentum at which  $\pi$ 's and  $K$ 's can be separated by the RICH technique.

However, RICH detectors seldom have too much signal, and some compromise on the value of  $n$  may be in order if another liquid is significantly more transparent. A large variety of fluorinated hydrocarbon liquids of excellent purity are available from the 3M Fluorinert Products Division. In particular they recommend that  $C_8F_{18}$  (called FC-104 by 3M) be considered if uv transparency is critical. The index of  $C_8F_{18}$  is quoted as being only 1.29, 0.02 larger than that of  $C_6F_{14}$ , and so seems still safely below  $\sqrt{2}$ .

We have evaluated a sample of  $C_8F_{18}$  with our spectrophotometer and it is indeed more transparent than  $C_6F_{14}$  down to 190 nm, the operating limit of our instrument. We are presently unable to address the critical issue of whether  $C_8F_{18}$  is transparent down to 170 nm, the cutoff of quartz windows. For this we propose to purchase a vacuum spectrophotometer to study the transparency of this and other liquids, as well as that of the windows for RICH counters.

### 1.2.2 Preparation of High Quantum-Efficiency Photocathodes

As remarked in section 3, only recently have we been able to produce CsI photocathodes at Princeton with extremely high quantum efficiency. Continuing efforts will be required to insure that these high efficiencies can be reproduced on a routine basis.

Various improvements to our vacuum-deposition system will no doubt be needed. We have certainly benefited from our recent conversion from an oil-diffusion pump to an oil-free molecular-drag/diaphragm pump combination. However, the oil-free pump has a rather low pumping speed and is more appropriate for our test chambers than for the relatively large volume of bell jar of the evaporator. We propose to purchase a Balzers TSH180H turbomolecular/molecular-drag/diaphragm pump combination for use with the vacuum evaporator (item A1 of the Budget Explanation Page) along with an ion-gauge controller to monitor the operating pressure (item A4).

### 1.2.3 Cosmic-Ray Test Chambers

There are no test beams available in the U.S. until summer 1993, when we will return to BNL. In the meanwhile cosmic ray can be used as test particles, albeit at a rather low rate. Our present test chambers at Princeton have cathodes of area only about 4 cm<sup>2</sup>, which leads to cosmic-ray event rates of only a few per hour when some directionality is required.

We therefore propose to construct a pair of test chambers with 20-cm-diameter cathodes (item A2). The mechanical design of these chambers is sketched in Fig. 1, and is based on the general features of the prototype chamber we tested at BNL earlier this year. Initially we will read each chamber out as a single large pad. We can easily calibrate the test chamber for single photons using our pulsed hydrogen lamp. Then the total number of Čerenkov photons can be measured even though rings are not resolved.

The test chambers will then be used to verify the improvements in Čerenkov-photon yield due to increased transparency of the radiator and enhanced quantum efficiency of the



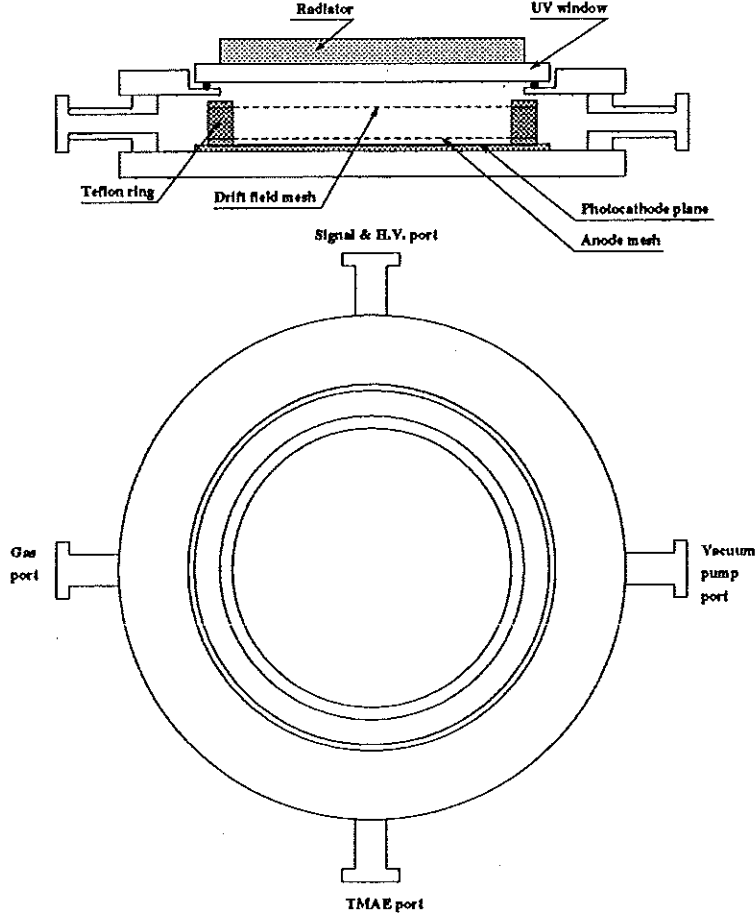


Figure 1: Sketch of the proposed test chambers for studies of Čerenkov yield and of time-of-flight at Princeton U.

photocathode.

#### 1.2.4 Semitransparent Photocathodes

We plan to explore the use of semitransparent photocathodes. These are standard in photomultiplier tubes, but have not yet been studied in the parallel-plate RICH detectors. A device with a semitransparent photocathode deposited on the quartz window would not need a wire-mesh anode. Thus we could avoid the  $\approx 25\%$  loss of light in the mesh, and also the problem of stretching the mesh uniformly over large areas.

#### 1.2.5 LiF Substrate

In present CsI photocathodes many of the photoelectrons are lost as their momentum points away from the surface. Some of these are likely recovered by scattering in a thick CsI layer. Although the photoabsorption depth in CsI is only a few hundred Angstroms, there is a slow rise in quantum efficiency for thicknesses up to  $1\text{ }\mu\text{m}$ , possibly due to favorable



backscattering.

We plan to try an alternative method of obtaining backscattering: use of thin CsI layers on a thin LiF (or NaF) substrate. Lithium fluoride has the largest bandgap energy ( $\approx 11$  V) of any alkali halide, which is much larger than the energy of photoelectrons of interest in RICH detectors. Hence we expect photoelectrons from CsI to be reflected back at a CsI-LiF interface.

If this hypothesis proves correct, the gain in quantum efficiency could be especially useful for semitransparent cathodes.

### 1.2.6 Spray-on Photocathodes

We would like to explore the viability of spraying CsI dissolved in methanol onto the cathode, rather than evaporating it as presently done. The spraying could be performed in a glove box (item A9) with a dry-N<sub>2</sub> atmosphere, avoided any exposure of the cathode to room air. Small-scale spraying tests at Fermilab are quite encouraging [12].

We propose to purchase a precision spray nozzle and controller (item A7), and construct an automated  $x$ - $y$  stage (item A8) to move the nozzle over the cathode in a controlled pattern. Past efforts using an air brush have not provided sufficient uniformity of the cathode thickness, and a better technique must be achieved.

### 1.2.7 Atmospheric-Pressure RICH Detectors with CsI

All chambers constructed with CsI photocathodes thus far have been built as vacuum vessels for low-pressure operation. If the transparency of the radiator can be extended down to 170 nm and very high quantum efficiencies achieved, there will be sufficient light that we can afford to pay the  $\approx 25\%$  penalty for operation at atmospheric pressure. This would greatly simplify the construction of large RICH detectors based on CsI photocathodes.

We will construct a prototype detector for atmospheric-pressure operation only, *i.e.*, it will not be a vacuum vessel. The first version would have only a single readout pad, as the main purpose is to explore construction techniques. Later versions would implement an array of pad for detection of Čerenkov rings.

The new test chambers should have an associated oil-free pump (item A3) and ion-gauge controller (item A4).

### 1.2.8 CsI Photocathodes for Time-of-Flight Counters

Parallel-plate chambers with CsI cathodes have excellent timing properties in principle: time resolutions of better than 100 ps should be achievable. Some effort was made at Fermilab in the last year to explore the use of these chambers as time-of-flight counters, but that work was not carried to a conclusion. We propose to pursue this topic further in the next year, using the new test chambers discussed in the previous section with cosmic rays as the test particles.

We will also extend our work on low-density CsI films, discussed in section 3.3, which have better electron transport properties than bulk-density material. The goal is to obtain 30 or more secondary-emission electrons from passage of a minimum-ionizing particle, which is not possible in full-density films. We must achieve greater control over the density of the



films ( $\sim 0.03 \text{ gm/cm}^3$  is desirable), for which the improved vacuum system of our evaporator (items A1 and A4) will be important.

### 1.2.9 Beam Tests

We will return to the BNL test beam in summer 1993 to test the various chambers described above the we have built this winter. We anticipate that in these tests we will demonstrate devices with 15-25 photoelectrons per ring, which would be fully viable as detectors in high-energy-physics experiments.

### 1.2.10 Infrastructure Support

As discussed further in sec. 2.7, an important part of our use of TNRLC funding in FY91 and FY92 has been toward infrastructure improvements. We wish to devote part of prospective FY93 funding in this manner.

In particular, we have hired an electrical engineer who has helped us establish a strong electronics CAD capability based on Mentor Graphics software running on Sun workstations. We propose 5 months of this engineer's salary in FY93 (item D1) to be funded by the present grant renewal. The use of the CAD workstations has been highly successful with both students and the electronics-group staff (five FastBus boards designed, fabricated and tested in the last 6 months) that we propose to add two more workstations (item B1).

We also propose to purchase several items of electronics (items B2-4 and C1-4) in support of the development of the fast RICH detectors. A PC computer, data acquisition system, power supplies, and trigger electronics will be used to establish the cosmic-ray test stand discussed in sec. 2.2.3. The fast pulser and oscilloscopes are needed to characterize the high-rate performance of the detectors.

## 1.3 Research Personnel

The proposed R&D program on particle identification will be pursued full-time by C. Lu, and part-time (in order of decreasing fraction of their time) by K. McDonald, E. Prebys, and D. Marlow. Two graduate students, V. Balasubramanian and Y. Zhu participate in the program at present. Participation by Princeton U. technical staff is mentioned in sec. 2.6.

## 1.4 Methodology

The clear test of success of detectors of elementary-particles is their successful operation in a high-energy particle beam. So our efforts in FY91 and FY92 have both included beam tests of prototype devices, and we anticipate further beam tests in FY93.

In preparation for these tests (in which the national accelerator labs contribute beam time and modest technical support free – a kind of matching funds!) we first maximize our understanding of the detectors on the test bench, using radioactive sources of charged particles, and photon sources (lamps).



## 1.5 Relevance to the SSC

As discussed in sec. 2.1, hadron identification is of particular interest to a possible  $B$ -meson physics program at the SSC. The high multiplicities and high rates at the SSC require detectors for particle identification with good segmentation and high-speed operation. RICH counters are well suited to high particle multiplicity, but past implementations have used readout schemes unsuitable for high rates. Hence new technologies must be developed, which is the motivation for the present proposal.

## 1.6 Institutional Commitment and Sources of Additional Support

Princeton U. and the DoE provide salary support for all physics researchers associated with this proposal. In addition the DoE high-energy-physics grant to Princeton provides salaries for a staff of a mechanical engineer, four mechanical technicians, and three electronics technicians; they work part-time in support of the R&D funded by the TNRLC at no direct cost to the Grant.

Princeton U. has provided three kinds of matching funds for the TNRLC grants in FY91 and FY92: funds from the Physics Department endowed research fund; funds from the Provost's office, and contribution of indirect costs on the salary (+ benefits) for the electrical engineer supported in part by the TNRLC grant. In FY93 only matching funds in the form of indirect costs will be available from Princeton U. for this proposal.

In addition we wish to note that the TNRLC funding has given us great leverage in obtaining special discounts from equipment vendors. These can properly be considered as industry-sponsored matching funds for our R&D program. The largest 'discount' in the past was from Mentor Graphics who awarded us a software grant of \$309k (list price) of CAD software in FY91. We receive free software upgrades from Mentor Graphics on a continuing basis. Sun Microsystems has extended us 50% matching funds (\$30k in FY91 and \$12k in FY92) on the purchase of the workstations to run the CAD software as one of us (P.D. Meyers) is a Presidential Young Investigator. We anticipate an additional \$30k discount from Sun in FY93.

## 1.7 Impact on Infrastructure of Science and Engineering

The TNRLC grants to Princeton in FY91 and FY92 have had an enormous effect in enhancing the technical infrastructure for high-energy physics at Princeton. We have purchased several major pieces of equipment that are extremely difficult to obtain (at universities) via historical funding trends by the DoE (our main source of support): a clean room, a (used) coordinate measuring machine, two lathes, three milling machines, a logic analyzer, a spectrum analyzer, a 20-GHz sampling oscilloscope. In addition, many smaller equipment items were purchased that are more typical of those obtainable via DoE HEP support, but which could not have been otherwise purchased under present funding restrictions.

These items represent an investment in infrastructure that will benefit our physics program for 10-15 years. The horizons for students entering our field are much broader because



of this, and their future contributions as mature physicists will be one to the greatest payoffs of the initiative of the TNRLC.

## 2 Research Accomplishments in FY91 and FY92

The largest component of our R&D effort sponsored by the TNRLC in FY91 was on precision tracking with gas-filled 'straw-tube' detectors. This work had already begun over two years ago under the auspices of the SSC Generic and Subsystem R&D programs. In FY92 our focus shifted to detectors for hadron identification based on ring imaging Čerenkov counters with solid CsI photocathodes, and (more speculatively) on time-of-flight counters using secondary emission in low-density CsI films. Also, we have applied part of our funding towards much-needed improvements to our technical infrastructure, as discussed in sec. 2.7.

### 2.1 Precision Straw-Tube Tracking

In FY91 our main R&D focus was on straw-tube tracking. Studies were of two types: bench tests to characterize single-electron avalanches [23], and a beam test of system performance [24].

The bench test exploited a technique to study the gas gain of a single electron ejected by a pulsed N<sub>2</sub> laser from aluminum walls of straw tubes. The Townsend avalanche coefficient, the electron-attachment coefficient, as well as the drift velocity were measured (using different test-chambers). Particular emphasis was placed on CF<sub>4</sub> gas mixtures whose high drift velocity and low diffusion are favorable for use at the SSC. These gases suffer from non-negligible electron attachment, however, as was studied by us in some detail.

The beam test was of a system of three 8 × 8 straw-tube modules equipped with bipolar VLSI amplifier/shapers designed at U. Penn in an AT&T process. Nineteen gas mixtures were studied at Fermilab, and the efficiency and resolution *vs.* impact parameter deduced. While we achieved  $\approx 100\ \mu\text{m}$  resolution with argon-ethane mixtures, the best observed in a CF<sub>4</sub> mixture are about 150  $\mu\text{m}$ .

Many of the techniques developed for study of straw tubes on the test bench were readily adapted in FY92 to study the gas gain in RICH detectors with parallel-plate avalanche chambers.

### 2.2 Particle Identification with Fast RICH Counters

#### 2.2.1 Beam Test of a RICH Prototype

In collaboration with N.S. Lockyer *et al.* of U. Pennsylvania we constructed and tested a low-pressure, parallel-plate pad-chamber with a cesium-iodide solid photocathode and 332 pads read out with SVX chips, sketched in Fig. 2. This detector is blind to minimum-ionizing particles, and sensitive to Čerenkov photons of wavelengths 170-210 nm. We observed an average of 5 photoelectrons per Čerenkov ring were detected using a 2-cm-thick radiator of liquid C<sub>6</sub>F<sub>14</sub> [18].

We are very encouraged with these results obtained in a BNL beam test. Three single-particle events are shown in Fig. 3 with struck pads indicated as squares. Each photoelectron



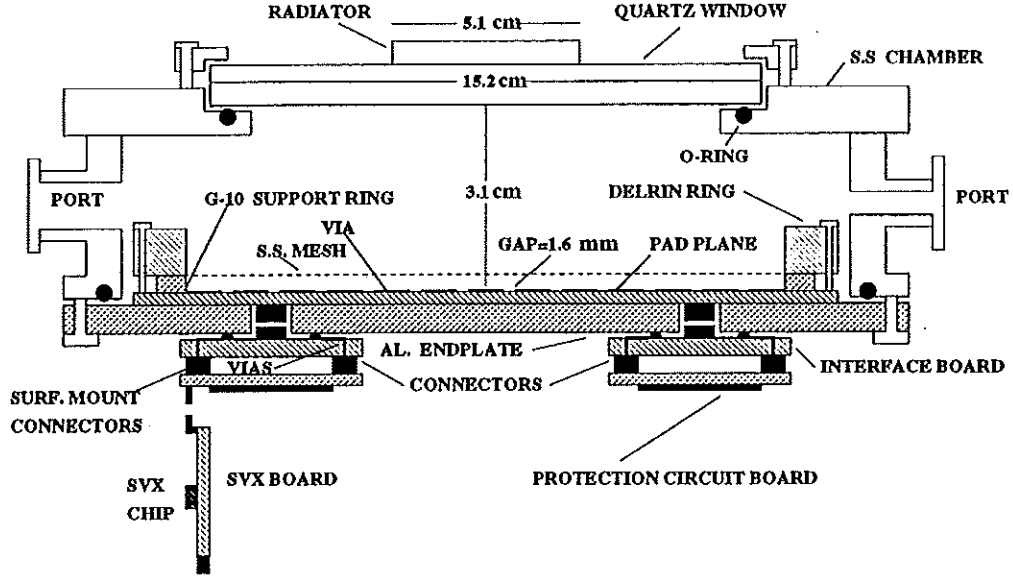


Figure 2: Schematic view of the prototype RICH detector showing the radiator, low-pressure gas volume, semitransparent steel-mesh anode, pad-plane cathode, and configuration of printed-circuit boards on which the SVX readout chips are mounted.

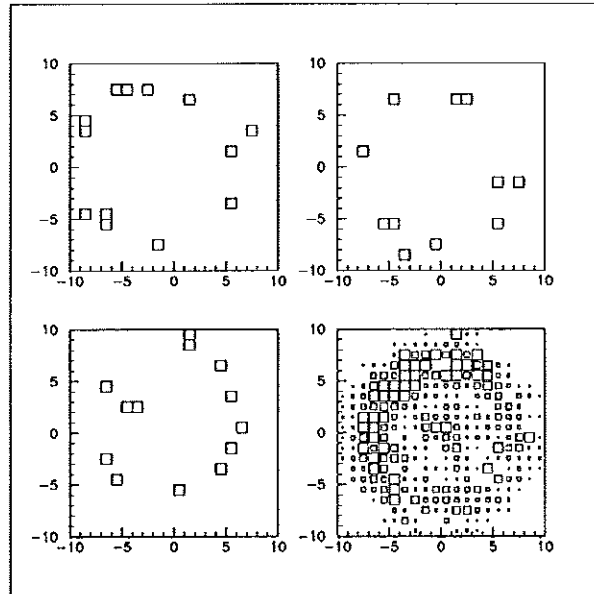


Figure 3: Three plots are single-particle events displaying obvious rings. The fourth plot shows a sum of events from a short run.



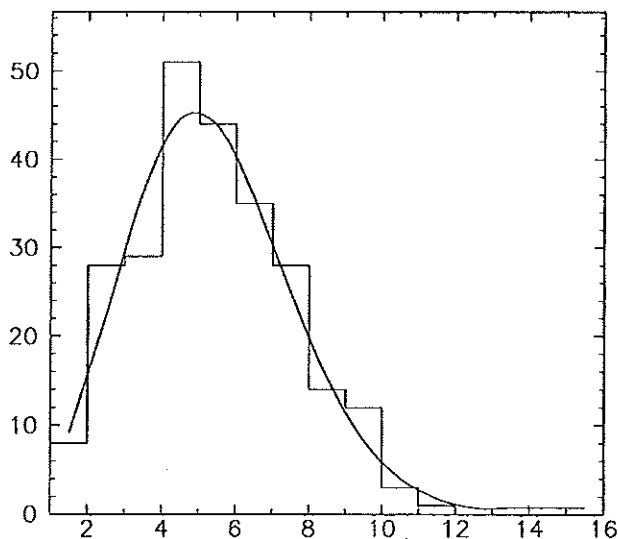


Figure 4: The spectrum of the number of detected photoelectrons per event from minimum-ionizing particles, fit to a Poisson distribution of mean 4.9.

typically excites one pad, and the ring is easily identified. Shown in the lower-right of Fig. 3 is the sum of hits over a short run. The area of each bin reflects the summed number of hits. The general outline of the rings are seen to be enhanced, although there is smearing due to the transverse size of the radiator. The nonuniform density of hits around the ring is possibly due to uneven gain across the surface of the pad plane which resulted from a warping of the anode support ring during heating. Note that roughly 10% of the rings have a hit in their center, which corresponds to the probability that a minimum-ionizing particle is detected.

We observed an average of 5 photons per Čerenkov ring as displayed in the histogram of the multiplicity of hits per ring in figure 4. We calculate the number of photoelectron per ring would be twenty if our photocathode had the high quantum efficiency reported by Anderson *et al.* [12]. The prospect of a factor of four improvement is the prime motivation of our research program in FY93.

The gas gain in the low-pressure parallel-plate chamber can be as high as  $10^6$ , but we typically operate at  $10^5$  gain. The wire mesh plane was easy to construct and the chamber operates even with small defects in the wire mesh caused by months of handling during the many photocathode evaporations. The data-acquisition system [20, 21] worked well during the test run.

In addition to participation in the construction and testing of the prototype RICH detector described above, we have made a number of benchtop studies of photocathodes, gas mixtures, and radiators.



## 2.2.2 Monte Carlo Simulation of the RICH Detector

To understand the various factors of the efficiency of the prototype RICH detector a simple Monte Carlo program has been written. Here we present some details discussed only briefly in ref. [18].

The following physical processes were included in the simulation:

1. The Čerenkov-light spectrum per unit length of radiator and unit wavelength interval is:

$$\frac{d^2 N}{d\lambda dL} = 2\pi\alpha \frac{\sin^2 \theta_C}{\lambda^2} = 4.58 \times 10^5 \frac{\sin^2 \theta_C}{\lambda^2},$$

where  $\lambda$  is in nm, and the radiator length  $L$  is in cm.

2. The index of refraction of the  $C_6F_{14}$  liquid radiator as a function of wavelength was taken as follows [4]:

$$n_{C_6F_{14}}(E) = 1.2733 + 9.3 \times 10^{-3}(E - 6),$$

where photon energy  $E$  is in eV. The Čerenkov angle for index 1.273 is  $38^\circ$ .

3. The wavelength interval for photon detection was taken as 170-220 nm, so the average number  $\bar{N}$  of Čerenkov photons per cm of radiator in this interval is

$$\bar{N} = 462.62 \sin^2 \theta_C = 179.37.$$

4. The actual number  $N$  of photons was Gaussian distributed with average  $\bar{N}$  and  $\sigma = \sqrt{\bar{N}}$ , and were randomly distributed along the track of a minimum-ionizing particle in the radiator.
5. The external transmission of  $C_6F_{14}$  was measured with a Perkin-Elmer Lambda 3 spectrophotometer within a region of 190-220 nm, and corrected for the reflection at the interfaces air-to-UV-window and liquid-to-UV-window to obtain the internal transmission. Due to the lack of a VUV spectrophotometer we were not able to measure the transmission for 170-190 nm. For  $\lambda < 190$  nm we used data from Arnold *et al.* [4], who report that the transmission of  $C_6F_{14}$  is not sensitive to the purification procedure in this region. The data points with a fitting curve are shown in Fig. 5. The  $C_6F_{14}$  was purified by passage through Oxisorb.

6. The refractive index of UV-grade fused silica was taken from the Melles-Griot catalog as:

$$n_Q^2 - 1 = \frac{0.6961663\lambda^2}{\lambda^2 - (0.0684043)^2} + \frac{0.4079426\lambda^2}{\lambda^2 - (0.1162414)^2} + \frac{0.8974794\lambda^2}{\lambda^2 - (9.896161)^2},$$

for  $\lambda$  in  $\mu\text{m}$ . A typical value is  $n_Q = 1.57$  at 190 nm.

7. The internal transmission of the UV-grade fused silica window was taken from the Melles-Griot catalog. The mean free path length  $\mu$  was taken as

$$\mu = \frac{1}{\ln(1 - 10^{3.07223 - 0.023856\lambda})},$$

with  $\lambda$  in nm.



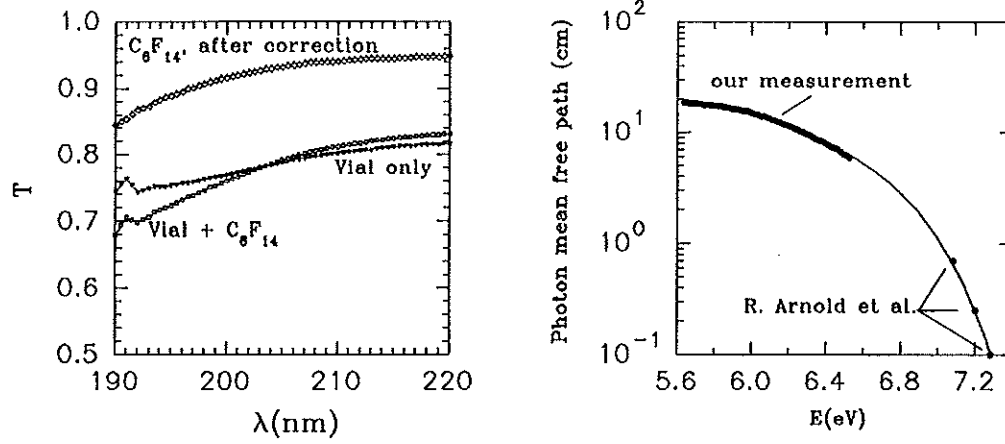


Figure 5: a) Spectrophotometer scans of transmission of  $C_6F_{14}$  liquid in a 1-cm-pathlength vial. b) The mean free path for uv light in  $C_6F_{14}$  as a function of photon energy. The three data points at high energy are from Arnold *et al.* [4].

8. The reflection of Čerenkov light on the interfaces between fused silica and air is governed by Fresnel's equations. Because the Čerenkov radiation is linearly polarized in the plane of incidence (containing the direction of observation and the path of the particle), the coefficient of reflection is

$$R_{\parallel} = \left[ \frac{n_t \cos \theta_i - n_i \cos \theta_t}{n_t \cos \theta_i + n_i \cos \theta_t} \right]^2.$$

The angles of Čerenkov light in vacuum, quartz and the  $C_6F_{14}$  radiator are related by

$$\sin \theta = n_Q \sin \theta_Q = n_{C_6F_{14}} \sin \theta_C, \quad \text{so that} \quad \theta \approx 52^\circ \quad \text{and} \quad \theta_Q \approx 30^\circ.$$

For both the vacuum-quartz and quartz-liquid interfaces we are very near the Brewster angle at which  $R_{\parallel}$  vanishes.

9. The transmittance of the anode mesh was considered as a constant. For normal incidence the transmittance was  $(0.9)^2 = 0.81$ , the square of the ratio of the spacing between wires to the spacing of wire centers. Čerenkov light is incident on the mesh at  $52^\circ$  from the normal, so the transmission factor in each projection  $(L' - a)/L'$  varies between 0.9 and 0.83. The combined transmission varies between  $(0.9)(0.83) = 0.75$  and  $(0.83)^2 = 0.69$ , and we take 0.72 as the average transmittance.
10. The quantum efficiency of the CsI photocathode was inferred from work of Anderson *et al.* [12], who report results with both methane and isobutane chamber gas. Our gas, ethane, is expected to have performance intermediate between these two gases, so we calculate for both methane and isobutane.



11. For each photoelectron ejected from the photocathode, a Townsend avalanche was generated according to Polya distribution [22] for the observed gas gain  $g$ :

$$P(g) = \left( \frac{b}{b-1} \frac{g}{\bar{g}} \right)^{b-1} e^{(b-1-bg/\bar{g})},$$

where  $\bar{g}$  is the mean gas gain, and  $b$  is a measure of the fluctuation in gain. We took  $\bar{g} = 10^5$ , and  $b = 1.5$  in our calculation. The threshold of the electronics was set at  $g = 2000$ .

The simulation of the RICH detector was carried out for methane and isobutane chamber gas and for four different radiator lengths from 1 to 4 cm. The various efficiency distributions used in our simulation are shown in Fig. 6. The total number of detected photons are shown in Fig. 7. For data collected at BNL with the RICH prototype we used a 2-cm-thick radiator. If we suppose ethane gas is close to isobutane in performance with a CsI photocathode, the expected number of hits per Čerenkov ring would be 20.

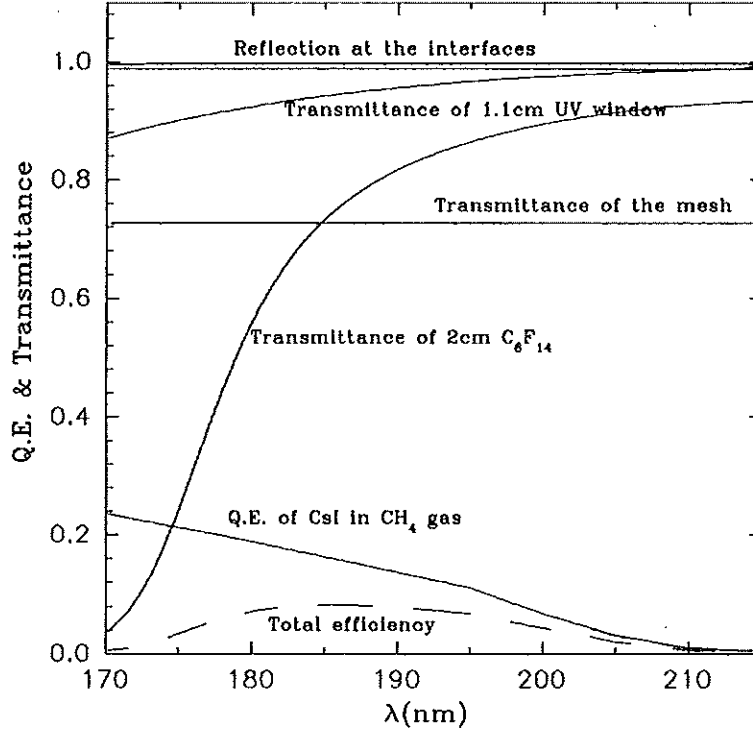


Figure 6: Various efficiency distributions that enter the RICH detector simulation.

### 2.2.3 Measurement of Quantum Efficiency of CsI Cathodes

At Princeton U. we have built a small facility to fabricate and test CsI photocathodes. The cathodes are evaporated in a Denton DV-502 vacuum evaporator equipped with a Balzers



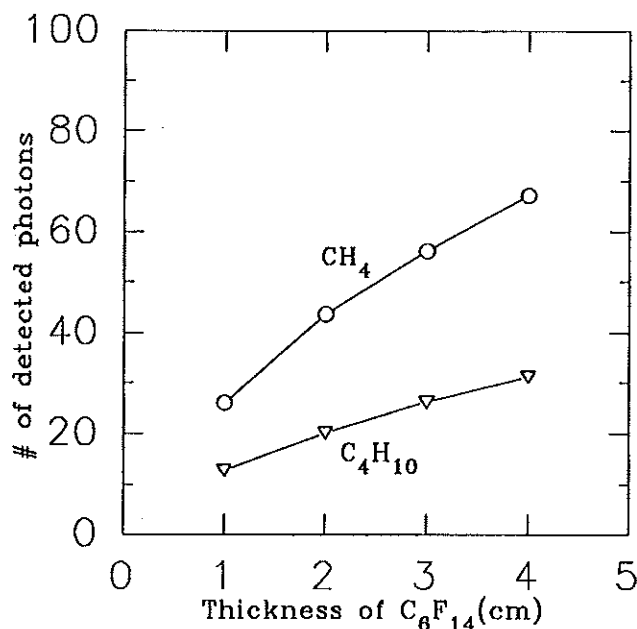


Figure 7: Prediction of the total number of detected photons in our RICH prototype if the photocathode had the quantum efficiency reported by Anderson *et al.* [12].

TPD020 molecular drag pump and oil-free diaphragm pump. The cathode substrate can be heated during evaporation by water piped in from a circulating temperature bath and/or by infrared lamp shining through the glass bell jar.

The quantum efficiency of the cathodes can be evaluated in a small test chamber shown in Fig. 8. UV light is derived from a pulsed hydrogen lamp (Hamamatsu) and the desired wavelength selected with a monochromator (Instruments SA model H1061). For studies down to 170-nm wavelength, the cutoff of uv-grade quartz, all light paths must be in nitrogen. The photocathode is mounted in a small parallel-plate chamber patterned after the work of Hoeneisen *et al.* [10], which permits use of TMAE photosensitive gas as the reference for quantum efficiency.

Only recently, and after considerable effort, have we produced photocathodes that approach the high quantum efficiencies reported by Anderson *et al.* [12]. Very exacting standards of care and cleanliness must be maintained during the fabrication procedure. Our best cathodes are made from pure CsI obtained in crystal form from Bicon Co. Figure 9 shows our measured quantum efficiency *vs.* wavelength for a cathode used with isobutane and with ethane gas at 20-torr pressures.

Older studies with a low-quantum-efficiency cathode permitted measurements of the optical transmission of methane, ethane and isobutane at wavelengths below 190 nm, at which our commercial spectrophotometer does not operate (due to photoabsorption by oxygen in the air). Figure 10 shows the transmission of uv light through the 2.5-cm-thick gas-filled chamber gap. This is not an absolute measurement, but shows that isobutane is much less transparent than ethane or methane below 175 nm.



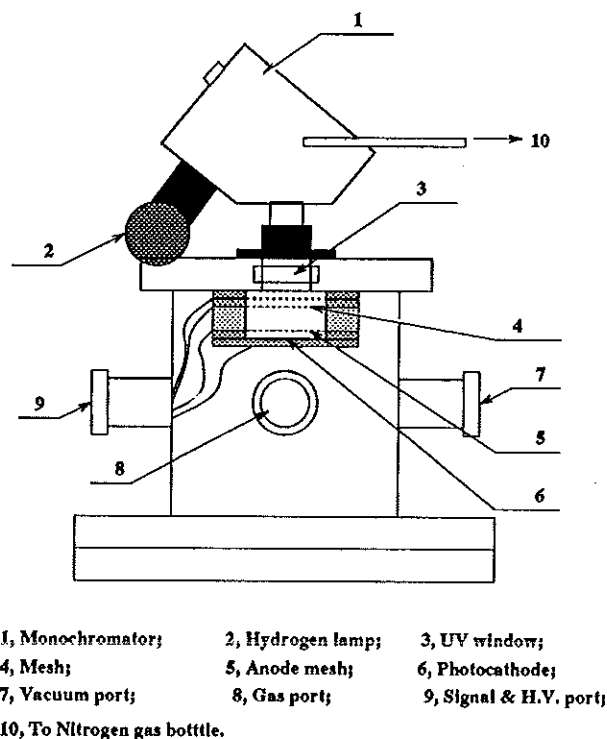


Figure 8: The test chamber for measurement of quantum efficiency *vs.* wavelength.

As the quartz cutoff is 170 nm, the maximum quantum efficiency in a RICH detector could be obtained with methane or ethane gas rather than isobutane – provided the radiator is also transparent at down to 170 nm. From Figure 5 we see that liquid  $C_8F_{14}$  does not satisfy this criterion. In the future we will investigate the use of  $C_8F_{18}$  as the radiator, since the vendor (3M Fluorinert Products, type FC-104) advises us this liquid is more transparent in the uv. A vacuum spectrophotometer will be required for these studies.

#### 2.2.4 Atmospheric-Pressure Operation

We have also studied the possibility of operating the CsI photocathode RICH detectors at atmospheric pressure [25]. This would greatly ease the difficulty of construction of large-scale detectors. However, as demonstrated by Anderson [19] several years ago, a gas at atmospheric pressure reflects up to 50% of the photoelectrons back onto the photocathode where they are lost. We have verified this for various helium gas mixtures, as shown in Fig. 11. Among possible admixtures of methane, ethane, isobutane,  $CO_2$ , or  $CF_4$  the most favorable choice appears to be isobutane for which the observed quantum efficiency of a CsI cathode in He/isobutane (95/5) at 760 torr is 80% of that for isobutane at 38 torr. This is likely sufficient for viable operation of a RICH detector.

The use of helium as the buffer gas retains the desirable feature that the detector is largely blind to minimum-ionizing particles. Thus far we have only studied this with a



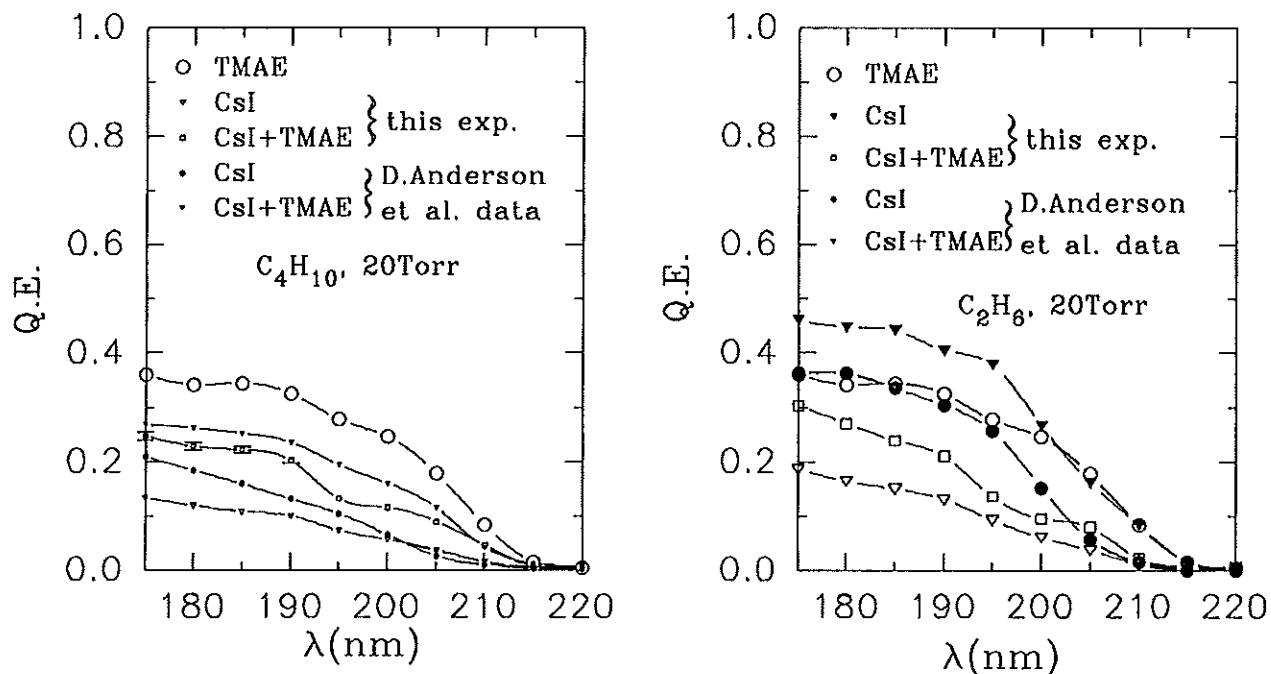


Figure 9: The quantum efficiency vs. wavelength for a CsI photocathode used with (a) isobutane gas and (b) ethane gas at 20-torr pressures. Also shown are results obtained by Anderson *et al.* [12].

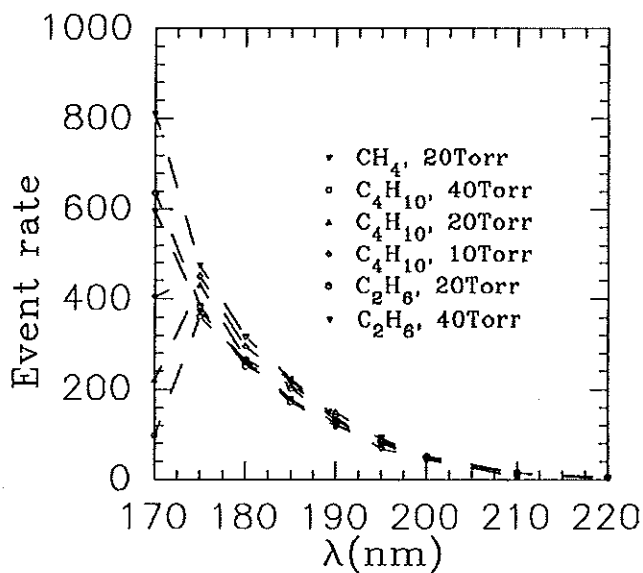


Figure 10: The relative transmission of light in methane, ethane and isobutane vs. wavelength. Isobutane is significantly less transparent than methane or ethane for 170-175 nm.



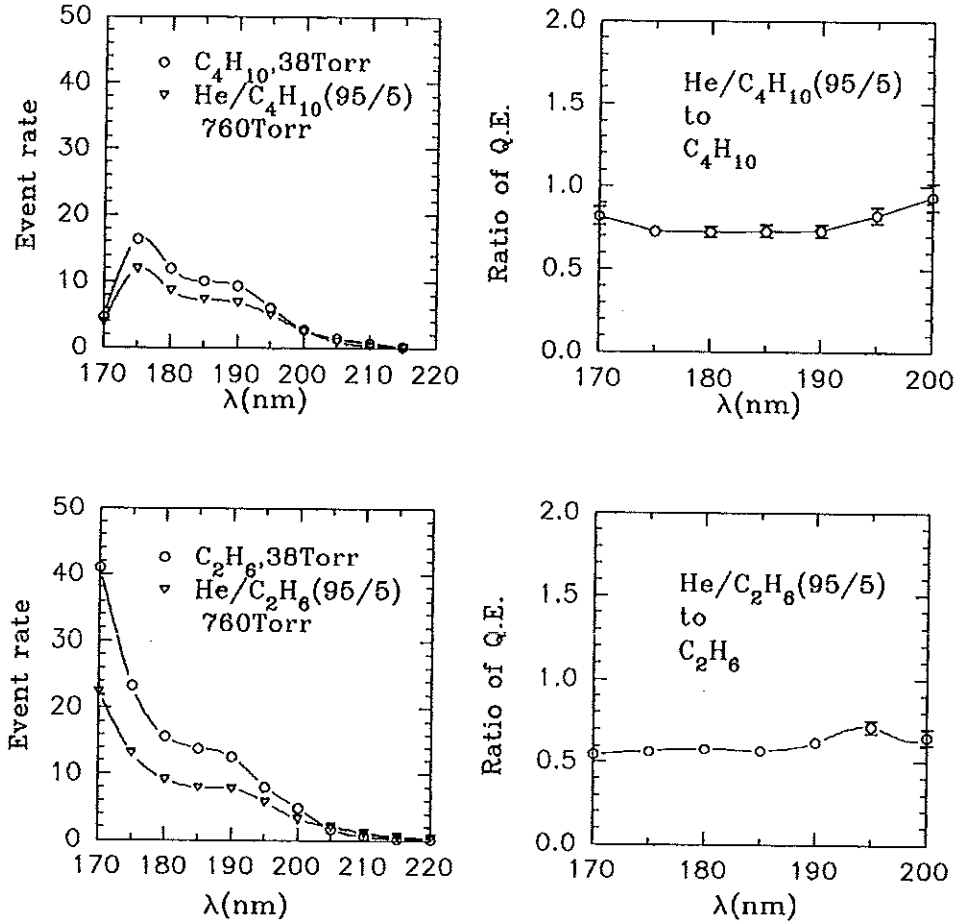


Figure 11: Comparison of observed quantum efficiency of a CsI photocathode in He/hydrocarbon gas mixtures at atmospheric pressure and hydrocarbon gases at 38 torr.

computer simulation of the gas avalanche based on measured data for the gain spectrum of single-photoelectron avalanches. Results are shown in Fig. 12 which indicates that the efficiency for minimum-ionizing particles is never higher than 40% for He gas mixtures of interest. Hence there will be no operational instabilities due to large avalanches induced by minimum-ionizing particles.

Another important issue for both parallel-plate chambers and wire chambers is the sensitivity of the gas gain to the spacing  $x$  between anode and cathode. From our measurements of the Townsend gain coefficient  $\alpha$  and fitted to the form  $\alpha = a/P + bE/P$  where  $P$  is the partial pressure of the gain gas, we infer the gain variation is  $\Delta G/G = aP\Delta x$ . The value of parameter  $a$  is smaller for isobutane than the other four gases we considered, which reinforces the potential of helium-isobutane mixtures for atmospheric-pressure operation.

Note also that if the gain gas has a high partial pressure, the gain is much more sensitive to mechanical variations in the chamber thickness. Thus helium gas mixtures (in which the helium contributes little to the gain) are more advantageous for stable operation of a



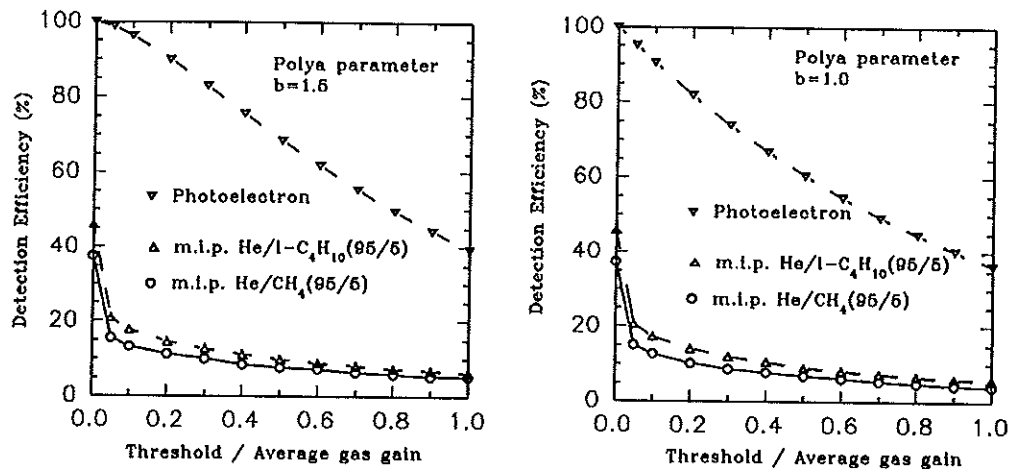


Figure 12: Computer simulation of the detection efficiency of a parallel-plate avalanche chamber with a CsI photocathode to minimum-ionizing particles and single photoelectrons for two He gas mixtures.

chamber than conventional atmospheric-pressure mixtures.

### 2.2.5 Effect of Water Vapor on CsI Photocathodes

While CsI does not react with oxygen, it is hygroscopic and the quantum efficiency of CsI photocathodes drops after exposure to water vapor. We have verified that heating the CsI cathode to  $\approx 40^\circ\text{C}$  for a period of time almost completely restores the quantum efficiency to that prior to exposure to water vapor, as shown in Fig. 13. Even exposure to 100% humidity leads to little or no permanent damage, if the photocathode is baked for one day thereafter.

## 2.3 Secondary Emission in Low-Density Semiconductor Films

In a RICH counter we prefer to be nearly insensitive to minimum-ionizing particles to have stable, high-gain operation of the detector for single photons. Even if there is little ionization of the chamber gas by a charged particle there may be creation of electron-hole pairs in the photocathode if CsI films are used. For the CsI photocathodes foreseen in RICH detectors this secondary emission is typically less than one electron liberated into the chamber gas per passing charged particle. However, it has been known for many years that secondary emission is enhanced in low-density semiconductor films [26].

CsI has bulk density of  $4.5 \text{ gm/cm}^3$ , and electronic structure very similar to xenon, so minimum-ionization is  $1.24 \text{ MeV}/(\text{gm/cm}^2)$ . Thus the energy deposition in a  $1\text{-}\mu\text{m}$ -thick layer of CsI (as often used in photocathodes for RICH detectors) is about  $560 \text{ eV}$ . Since the work function of CsI is approximately  $5.6 \text{ eV}$ , we might naively expect of order 100 electrons (so-called secondary-emission electrons) to emerge from  $1\text{-}\mu\text{m}$  layer of CsI when a minimum-ionizing particle passes through. Empirically, less than one electron is observed. This is partly due to the ionization energy being dissipated in other forms than conduction



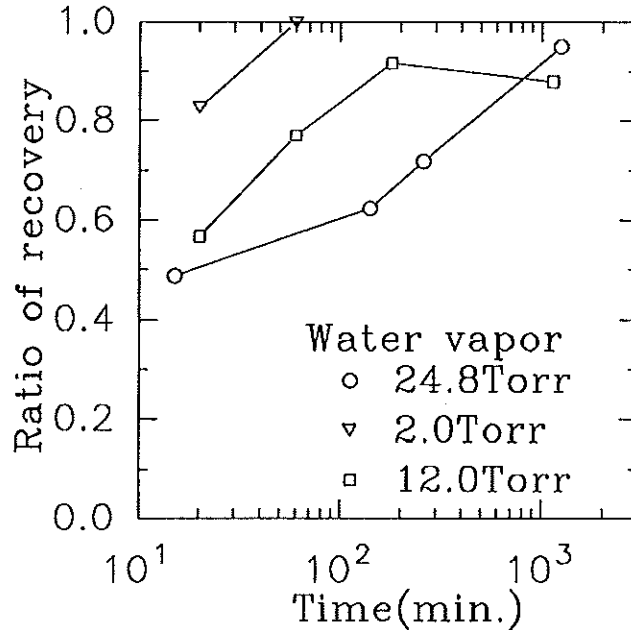


Figure 13: Recovery of the quantum efficiency of a CsI photocathode after exposure to water vapor as a function of time of heating at 40°C.

electrons, but also in large part due to poor electron transport. The low-density films apparently improve the electron transport dramatically.

We have verified the results of Goetze *et al.* [26] for KCl films via a Senior Thesis [27]. Then following the work of Bateman and Apsimon [28] we examined CsI films, and confirmed that it is much superior to KCl in secondary-emission yield.

To study the secondary emission we constructed two test setups in which electrons are photoejected from a cathode and accelerated to several kilovolts before impinging on a low-density CsI film. Figure 14 shows an arrangement using a (continuous) deuterium lamp, and Fig. 15 shows a setup using a pulsed N<sub>2</sub> laser so that the secondary emission signal can be time-resolved. From the variation of signal with accelerating voltage we infer that 3 keV of energy was deposited in our films by the electrons.

A result that requires further study is that the apparent secondary-emission yield is much higher with the continuous light source than with the pulsed laser, as shown in Fig. 16a. Even taking the lower yield as the correct one, secondary emission factors as high as 50 were observed, corresponding to 60 eV of deposited energy per secondary electron. This is quite encouraging for the detection of minimum-ionizing particles, and we plan to continue our studies.

### 3 References

- [1] For a review, see K.T. McDonald, *Six Ways to Measure CP-Violating Phases in B Decays*, Princeton/HEP/92-09 (Sept. 20, 1992).



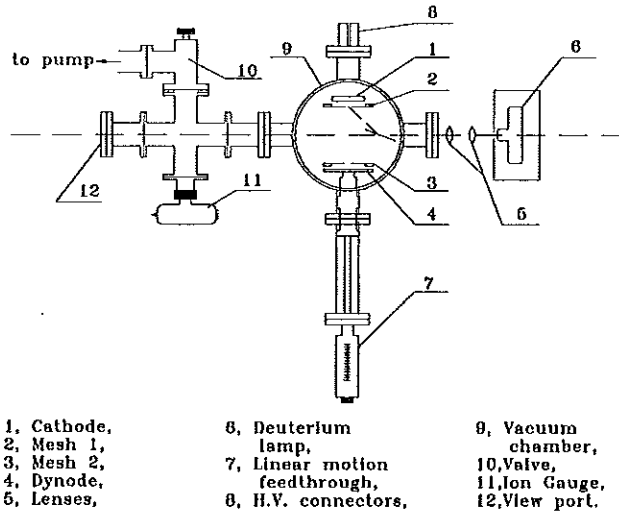


Figure 14: Setup to study secondary emission in low-density CsI films, using a deuterium lamp to photoject electrons that are accelerated to several kV before hitting the CsI film.

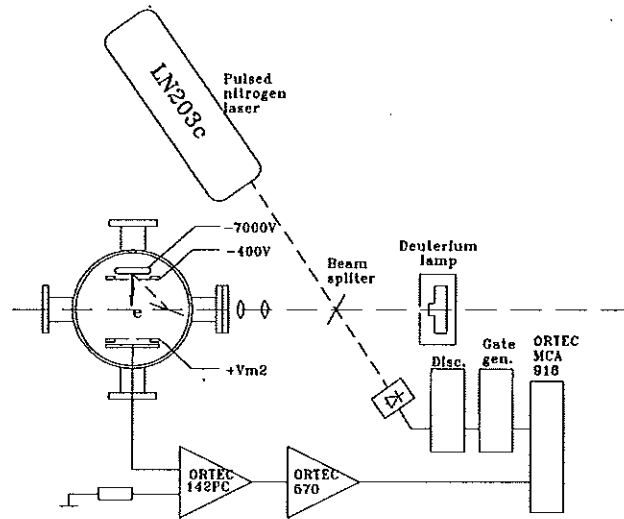


Figure 15: Setup to study secondary emission in low-density CsI films, using a pulsed  $N_2$  to photoject electrons that are accelerated to several kV before hitting the CsI film.

- [2] J. Séguinot and T. Ypsilantis, *Photo-ionization and Čerenkov Ring Imaging*, Nucl. Instr. and Meth. **142** (1977) 377.
- [3] D.W.G.S. Leith, *Status of Čerenkov Ring Imaging Systems*, Nucl. Instr. and Meth. **A265** (1988) 120.
- [4] R. Arnold *et al.*, *A Ring Imaging Čerenkov Detector for the Delphi Barrel RICH Prototype* Nucl. Instr. and Meth. **A270** (1988) 255, 289.



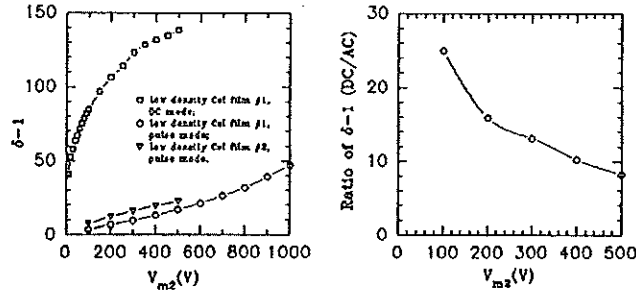


Figure 16: a) The observed ratio of secondary emission current to primary current as a function of voltage on the collector for both continuous and pulsed sources of primary electrons. b) The ratio of secondary currents for continuous and pulsed secondary emission.

- [5] A. Breskin *et al.*, *In Beam Performance of a Low-Pressure UV RICH Detector*, IEEE Trans. Nucl. Sci. 35 (1988) 404.
- [6] V. Vasileiadis *et al.*, *Development of a RICH Detector for Ultrarelativistic Heavy Ion Collisions*, Nucl. Instr. and Meth. A289 (1990) 618.
- [7] G.B. Coutrakon, B. Biggs and S. Dhawan, *Ring Imaging Čerenkov Detector Prototype Results*, IEEE Trans. Nucl. Sci. 33 (1986) 205.
- [8] A.H. Sommer, *Photoemissive Materials*, Wiley (New York, 1968).
- [9] L. Heroux, W.J. McMahon and H.E. Hinteregger, *The Influence of Cathode Thickness and Aging on the Photoelectric Yields of LiF and CsI in the xuv*, Appl. Opt. 5 (1966) 1338.
- [10] B. Hoeneisen, D. F. Anderson and S. Kwan, *A CsI-TMAE Photocathode with Low-Pressure Readout for RICH*, Nucl. Instr. and Meth. A302 (1991) 447.
- [11] S. Kwan and D.F. Anderson, *A Study of the CsI-TMAE Photocathode*, Nucl. Instr. and Meth. A309 (1991) 190.
- [12] D.F. Anderson *et al.*, *Properties of CsI and CsI-TMAE Photocathodes*, Fermilab-Conf-92/13 (June 1992), accepted for publication in Nucl. Instr. and Meth.
- [13] V. Peskov *et al.*, *Liquid and Solid Organic Photocathodes*, Nucl. Instr. and Meth. A269 (1988) 149.
- [14] J. Séguinot *et al.*, *Reflective UV Photocathodes with Gas-Phase Electron Extraction: Solid, Liquid, and Adsorbed Thin films*, Nucl. Instr. and Meth. A297 (1991) 133.
- [15] G. Charpak *et al.*, *Investigation of Operation of a Parallel-Plate Avalanche Chamber with a CsI Photocathode Under High Gain Conditions*, Nucl. Instr. and Meth. A307 (1991) 63.
- [16] V. Dangendorf *et al.*, Nucl. Instr. and Meth. A289 (1990) 322.
- [17] V. Dangendorf *et al.*, *Progress in Ultrafast CsI-Photocathode Gaseous Imaging Photomultipliers*, Nucl. Instr. and Meth. A308 (1991) 519.
- [18] N.S. Lockyer *et al.*, *Observation of Čerenkov Rings Using a Low-Pressure Parallel-Plate Chamber and a Solid Cesium-Iodide Photocathode*, UPR-0217E, Princeton/HEP/92-08 (Oct. 1992).
- [19] D.F. Anderson *et al.*, *Coupling of a BaF<sub>2</sub> Scintillator to a TMAE Photocathode and a Low-Pressure Wire Chamber*, Nucl. Instr. and Meth. 217 (1983) 217.
- [20] S. Kleinfelder *et al.*, *A Flexible 128 Channel Silicon Strip Detector Instrumentation Integrated Circuit with Sparse Data Readout*, IEEE Trans. Nucl. Sci. 35 (1988) 171.



- [21] F.A. Kirsten and C. Haber, *A Versatile, Programmable Control and Data Acquisition System for Complex Integrated Circuits*, IEEE Trans. Nucl. Sci. **37** (1990) 288.
- [22] J. Byrne, *Statistics of the Electron Multiplication Process in Proportional Counters*. Proc. Roy. Soc. Edin. **66A** (1962) 33.
- [23] W.S. Anderson *et al.*, *Electron Attachment, Effective Ionization Coefficient, and Electron Drift Velocity for CF<sub>4</sub> Gas Mixtures*, to appear in Nucl. Instr. and Meth.
- [24] J. Heinrich, *BCD Straw Test at Fermilab November-December 1991*, (April 14, 1992).
- [25] C. Lu, K.T. McDonald and Y. Zhu, *Helium Gas Mixtures for RICH Detectors with CsI Photocathodes*, Princeton/HEP/92-12 (October 1992, submitted to Nucl. Instr. and Meth.).
- [26] G.W. Goetze, A.H. Berio and M. Green, *Field-Enhanced Secondary Electron emission from Films of Low Density*, J. Appl. Phys. **35** (1964) 482.
- [27] E.R. Dunn, *Secondary Electron Emission from Low-Density Films and its Implication for Particle Detectors*, Princeton U. Senior Thesis (April 24, 1992).
- [28] J.E. Bateman and R.J. Apsimon, *A New Photocathode for X-Ray Image Intensifiers Operating in the 1-50 keV Region*, Adv. E. E. Phys. **52** (1979) 189.



## 4 Resumé of Kirk T. McDonald

Born: October 20, 1945, California

### Education:

1966 U. Arizona B.A. (Physics and Mathematics, Highest Honors)

1972 Caltech Ph.D. (Physics)

### Professional Employment:

1972-74 CERN Research Scientist

1975-76 U. Chicago Enrico Fermi Fellow

1976-80 Princeton U. Assistant Professor

1980-85 Princeton U. Associate Professor

1985- Princeton U. Professor

### Recent publications:

1. (with C. Biino *et al.*), *An Apparatus to Measure the Structure of the Pion*, Nucl. Instr. & Meth. **A243**, 323 (1986).
2. (with W.C. Louis *et al.*), *Upper Limits on the Decay  $D^0 \rightarrow \mu^+ \mu^-$  and on  $D^0$ - $\bar{D}^0$  Mixing*, Phys. Rev. Lett. **56**, 1027 (1986).
3. (with J.P. Alexander *et al.*), *Longitudinal Photon Polarization in Muon Pair Production at High  $x_F$* , Phys. Rev. D **34**, 315 (1986).
4. (with I.-H. Chiang *et al.*), *Search for Exclusive  $J/\psi$  Production*, Phys. Rev. D **34**, 1619 (1986).
5. (with K.D. Bonin *et al.*), *Observation of Interference Between Čerenkov and Synchrotron Radiation*, Phys. Rev. Lett. **57**, 2264 (1986).
6. (with C. Biino *et al.*),  *$J/\psi$  Longitudinal Polarization from  $\pi N$  Interactions*, Phys. Rev. Lett. **58**, 2523 (1987).
7. *Design of the Laser-Driven RF Electron Gun for the BNL Accelerator Test Facility*, IEEE Trans. Electron Devices, **35**, 2052 (1988).
8. (with J.S. Conway *et al.*), *Experimental Study of Muon Pairs Produced by 252-GeV Pions on Tungsten*, Phys. Rev. D **39**, 92 (1989).
9. (with J.G. Heinrich *et al.*), *Measurement of the Ratio of Sea to Valence Quarks in the Nucleon*, Phys. Rev. Lett. **63**, 356 (1989).
10. (with C. Farina and A. Tort), *Right and Wrong Use of the Lenz Vector for Non-Newtonian Potentials*, Am. J. Phys. **58**, 540 (1990).
11. *Motion of a Leaky Tank Car*, Am. J. Phys. **59**, 813 (1991).
12. (with J.G. Heinrich *et al.*), *Higher Twist Effects in the Reaction  $\pi^- N \rightarrow \mu^+ \mu^- X$  at 253 GeV/c*, Phys. Rev. D **44**, 1909 (1991).
13. (with W.S. Anderson *et al.*), *Electron Attachment, Effective Ionization Coefficient, and Electron Drift Velocity for  $CF_4$  Gas Mixtures*, to appear in Nucl. Instr. and Meth.
14. (with N.S. Lockyer *et al.*), *Observation of Čerenkov Rings Using a Low-Pressure Parallel-Plate Chamber and a Solid Cesium-Iodide Photocathode*, UPR-0217E, Princeton/HEP/92-08 (Oct. 1992), submitted to Nucl. Instr. and Meth.